Inorganic Chemistry

ARTICLE

pubs.acs.org/IC

Thermodynamic and Kinetic Studies on Novel Dinuclear Platinum(II) Complexes Containing Bidentate *N,N*-donor ligands

Stephanie Hochreuther,[†] Ralph Puchta,[†,‡] and Rudi van Eldik[†,*]

[†]Inorganic Chemistry, Department of Chemistry and Pharmacy, University of Erlangen-Nürnberg, Egerlandstr. 1, 91058 Erlangen, Germany

[‡]Computer Chemistry Center, Department of Chemistry and Pharmacy, University of Erlangen-Nürnberg, Nägelsbachstr. 25, 91052 Erlangen, Germany

Supporting Information

ABSTRACT: A series of novel dinuclear platinum(II) complexes were synthesized with bidentate nitrogen donor ligands. The two platinum centers are connected by an aliphatic chain of variable length. The selected chelating ligand system should stabilize the complex toward decomposition. The pK_a values and reactivity of four synthesized complexes, viz. $[Pt_2(N^1, N^4\text{-bis(2-pyridylmethyl)-1,4-butanediamine})(OH_2)_4]^{4+}$ (**4NNpy**), $[Pt_2(N^1, N^6\text{-bis(2-pyridylmethyl)-1,6-hexanediamine})(OH_2)_4]^{4+}$ (**6NNpy**), $[Pt_2(N^1,N^8\text{-bis(2-pyridylmethyl)-1,8-octanediamine})(OH_2)_4]^{4+}$ (**8NNpy**), and $[Pt_2(N^1,N^{10}\text{-bis(2-pyridylmethyl)-1,10-decanediamine})(OH_2)_4]^{4+}$ (**10NNpy**), were investigated. This system is of special interest because only little is known about the substitution behavior of dinuclear platinum complexes that contain a bidentate chelate that forms part of the aliphatic bridging ligand. Spectrophotometric acid−base titrations were performed to determine the pK_a values of the coordinated water ligands. The substitution of coordinated water by thiourea was studied under pseudofirst-order conditions as a function of nucleophile concentration, temperature, and pressure, using stopped-flow techniques and UV−vis spectroscopy. The results for the dinuclear complexes were compared to those for the corresponding mononuclear reference complex $[Pt(aminomethylpyridine)(OH_2)_2]^{2+}$ (**monoNNpy**), by which the effect of increasing the aliphatic chain length on the bridged complexes could be investigated. The results indicated that there is a clear interaction between the two platinum centers, which becomes weaker as the chain length between the metal centers increases. In addition, quantum chemical calculations were performed to support the interpretation and discussion of the experimental data.

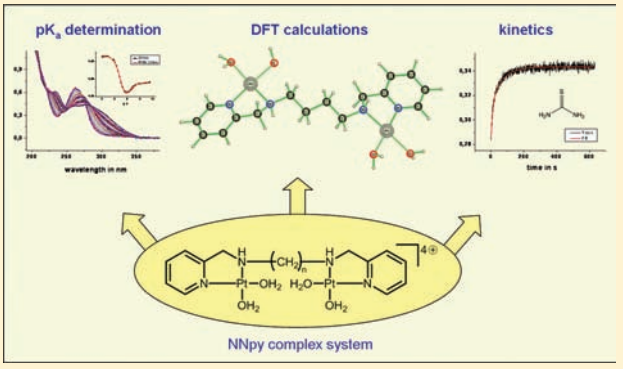

INTRODUCTION

In 1969, Barnet Rosenberg discovered the cytostatic activity of *cis*-diamminedichloroplatinum(II) − cisplatin − by chance.[1] Cisplatin is nowadays used worldwide in the treatment of testicular and ovarial cancer and is increasingly used against cervical, bladder, and head/neck tumors.[2] Following the example of cisplatin, thousands of platinum-containing compounds have been synthesized and evaluated as potential antitumor drugs but only a few compounds reached clinical applications, viz. carboplatin or oxaliplatin.[3] The development of new platinum compounds always continues, in the hope to suppress side effects, to overcome drug resistance during therapy and to afford a broader range of applications.[4] As known for several years,[5] a subsequent reaction with DNA will occur inside the nucleus, which results in a kink in the DNA structure and consequently leads to apoptosis of the cell or to reparation of the DNA by cutting out platinum and resynthesizing at the open sites.[6] This possibility of reparation of the platinated DNA leads to drug resistance and big efforts are still made to create novel platinum-containing compounds to reduce such cisplatin and carboplatin resistance, which may also violate the classical structure−activity relationship.[7] Nicholas Farrell set a milestone in developing new nonclassical platinum compounds. Farrell and co-workers invented polynuclear platinum compounds, for example the trinuclear **BBR3464** or the dinuclear system **(2,2/c,c-bn)** (Figure 1).[8−12]

The structure of **BBR3464** can be described as two *trans*-$[PtCl(NH_3)_2]^+$ units connected by a noncovalent tetraamine $[Pt(NH_3)_2\{H_2N(CH_2)_6NH_2\}_2]^{2+}$ unit. This agent was one of the first platinum drugs not based on the classical cisplatin structure and has presently entered phase II clinical trials. Unfortunately, low activity did not support further evaluation.[13] The structure of the dinuclear system **(2,2/c,c-bn)** can be described as $[\{cis\text{-}PtCl_2(NH_3)\}_2(diamine)]$ and belongs to a bidentate coordination sphere system compared to **BBR3464**.[9−11] Polynuclear complexes were developed to form noticeably different DNA adducts than cisplatin and carboplatin. The cross-links being formed involve mainly both strands of the DNA and are therefore supposed to be less susceptible to repair as both strands are affected by the damage.[14] As a consequence, those bis(platinum) complexes

Received: May 30, 2011
Published: August 01, 2011

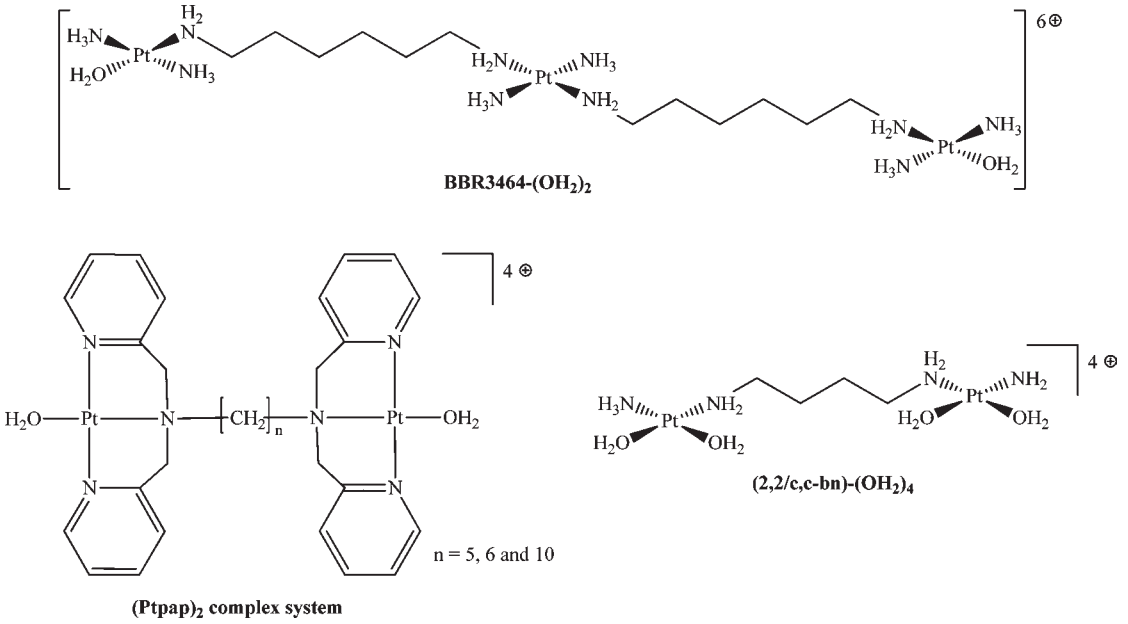

Figure 1. Schematic structures of a series of important polynuclear Pt(II) complexes and their abbreviations.

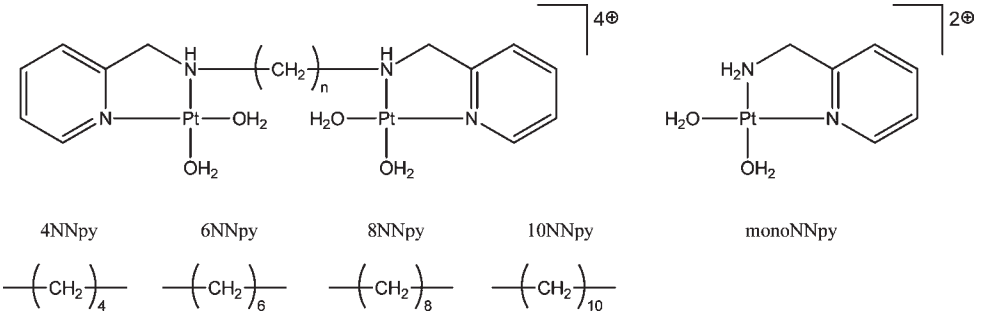

Figure 2. Schematic structures and abbreviations used for the studied complex system.

such as **(2,2/c,c-bn)** containing two Pt(amine)$_2$ units linked by a variable-length diamine chain are of chemical and biological interest because they show high activity against tumor cell lines resistant to cisplatin.[11] In this report, the work of Ertürk et al. was pursued.[15,16] He prepared dinuclear Pt(II) systems with monodentate coordination spheres. The two Pt(II) centers were coordinated by a tridentate bis(pyridylmethyl)amine unit and linked through an aliphatic chain (**(Ptpap)$_2$** as seen in Figure 1).

The platinum compounds presented in this work are also dinuclear but, compared to the complexes studied before, they consist of a bidentate ligand, which results in two vacant coordination positions as possible DNA binding sites. Furthermore, the dinuclear systems obey the structure−activity relationship, which requires at least one N−H moiety in the structure.[17−19] Figure 2 shows the Pt(II) complexes used in the present study (**NNpy** system). The dinuclear compounds include a chelating ligand system, namely a picolylamine unit. The two Pt(II) centers are connected by an aliphatic chain of variable length. The length of the chains, the two nitrogen donors, and the presence of a pyridine unit give the dinuclear Pt(II) compounds their abbreviations, viz., **4NNpy**, **6NNpy**, **8NNpy**, **10NNpy**, and **monoNNpy**, for the mononuclear reference complex without a bridging element, respectively. Because it is known[9−11] that the mode of DNA binding of dinuclear Pt complexes with bidentate coordination spheres is a complex area including interstrand cross-links (by each Pt center binding to opposite strands) and intrastrand cross-links (by cisplatin-like binding to two vicinal bases on a single strand), we tried to create a new dinuclear system to improve structural disadvantages of for instance **(2,2/c,c-bn)** and **BBR3464**, where primary am(m)ine ligands are used. However, it has been shown[20] that these complexes easily react with sulfur-containing nucleophiles, which leads to the release of the bridging ligand, decomposition of the complex, and therefore loss of cytostatic activity. The major structural difference of the complexes used in this study compared to **(2,2/c,c)** and **BBR3464** is the use of a chelating ligand system instead of primary am(m)ines. We expected that the chelating system will stabilize the complexes toward decomposition.

Naturally, the desired reaction is the binding of the Pt drug to the DNA to form DNA adducts, which are responsible for the cytostatic activity.[2,7] But, inside the cell many different nucleophiles are present, particularly sulfur-containing compounds, which often react with the Pt complex as reported recently.[20] In this work, we focus on the nature of the substitution reactions

dx.doi.org/10.1021/ic201151h |*Inorg. Chem.* 2011, 50, 8984–8996

with thiourea as a strong sulfur-containing nucleophile and their dependence on the chain length of the complexes. We report thermodynamic (pK_a values) and kinetic (rate constants) information on the complex system and used quantum chemical calculations to support the interpretation of the experimental results.

EXPERIMENTAL SECTION

Chemicals. The ligand 2-aminomethylpyridine, picolinaldehyde, the alkyl diamines, trifluoromethanesulfonic (triflic) acid, silver triflate, and thiourea were purchased from Acros Organics. Potassium tetrachloroplatinate(II) was purchased from Strem Chemicals. All other used chemicals were of the highest purity commercially available and were used without further purification. For all preparations of aqueous solutions, ultra pure water was used.

Preparation of the (*N*,*N*)-Ligand System. The ligands N^1,N^4-bis(2-pyridylmethyl)-1,4-butanediamine (**1**), N^1,N^6-bis(2-pyridylmethyl)-1,6-hexanediamine (**2**), N^1,N^8-bis(2-pyridylmethyl)-1,8-octanediamine (**3**), and N^1,N^{10}-bis(2-pyridylmethyl)-1,10-decanediamine (**4**) were synthesized following a general literature procedure:[21] To a solution of 10 mmol picolinaldehyde (1 mL) in 20 mL absolute methanol, 5 mmol of the corresponding diamine were added under nitrogen atmosphere. The resulting solution was stirred at 80 °C for at least 2 h. After cooling the solution to 0 °C (ice bath), 12.5 mmol solid sodium borohydride were added slowly within 45 min so that the temperature did not exceed 5 °C. In a final step, the solution was heated to 100 °C for 1 h. It was then cooled to room temperature and slowly diluted with 50 mL cold water to destroy excess sodium borohydride. Subsequently, the water/methanol mixture was extracted with dichloromethane (3 × 20 mL) and the combined organic layers were dried over anhydrous sodium sulfate. After evaporation of the solvent, the crude products (ligands **1**−**4**) were obtained as viscous orange oils. The organic compounds were converted into their corresponding hydrochloride salts to facilitate the handling of the ligands. The purification of the salts through recrystallization is most suitable, fast, and leads to pure (elemental analysis) compounds. Furthermore, the hydrochloride salts have the advantage of perfect water solubility, which is important because the reaction medium for K_2PtCl_4 is typically water. Therefore, the crude organic ligands were dissolved in sparse diethyl ether, cooled to 0 °C, and treated dropwise with 5 M HCl solution (20 mmol, 4 mL). The resulting off-white precipitate was recrystallized from water/methanol (1:1), giving white solids (**1*HCl**, **2*HCl**, **3*HCl**, and **4*HCl**) in all cases.

1*HCl: Yield: 1.28 g (3.08 mmol, M = 416.22 g/mol, 62%). Anal. Calcd for $C_{16}H_{26}Cl_4N_4$: C, 46.17; H, 6.30; N, 13.46%. Found: C, 46.14; H, 6.45; N, 13.33%. ^{1}H NMR (300.13 MHz, dmso-d_6, 298.2 K): δ 9.51 (br s, 2H), δ 8.72 (dd, $^3J_{HH}$ = 5.3 Hz, $^4J_{HH}$ = 1.6 Hz, 2H), δ 8.21 (dt, $^3J_{HH}$ = 7.9, $^3J_{HH}$ = 7.8 Hz, $^4J_{HH}$ = 1.6 Hz, 2H), δ 7.85 (d, $^3J_{HH}$ = 7.9 Hz, 2H), δ 7.72 (dd, $^3J_{HH}$ = 5.3 Hz, $^3J_{HH}$ = 7.8 Hz, 2H), δ 4.55 (s, 4H), δ 3.05 (t, $^3J_{HH}$ = 7.7 Hz, 4H), δ 1.75 (m, 4H). ^{13}C NMR (75.48 MHz, dmso-d_6, 298.2 K): δ 149.05, 146.65, 142.97, 126.53, 126.48, 49.06, 47.22, 23.20.

2*HCl: Yield: 1.01 g (2.71 mmol, M = 371.35 g/mol, 54%). Anal. Calcd for $C_{18}H_{28}Cl_2N_4$: C, 58.22; H, 7.60; N, 15.09%. Found: C, 58.43; H, 7.69; N, 15.13%. ^{1}H NMR (300.13 MHz, dmso-d_6, 298.2 K): δ 9.51 (br s, 2H), δ 8.72 (dd, $^3J_{HH}$ = 5.3 Hz, $^4J_{HH}$ = 1.6 Hz, 2H), δ 8.21 (dt, $^3J_{HH}$ = 7.9, $^3J_{HH}$ = 7.8 Hz, $^4J_{HH}$ = 1.6 Hz, 2H), δ 7.85 (dd, $^3J_{HH}$ = 7.9 Hz, $^4J_{HH}$ = 0.9 Hz, 2H), δ 7.72 (ddd, $^3J_{HH}$ = 5.3 Hz, $^3J_{HH}$ = 7.8 Hz, $^4J_{HH}$ = 0.9 Hz, 2H), δ 4.55 (s, 4H), δ 3.05 (t, $^3J_{HH}$ = 7.7 Hz, 4H), δ 1.75 (m, 4H). ^{13}C NMR (67.8 MHz, dmso-d_6, 298.2 K): δ 148.17, 145.78, 142.09, 125.66, 125.61, 48.19, 46.35, 22.33.

3*HCl: Yield: 1.79 g (3.79 mmol, M = 472.32 g/mol, 76%). Anal. Calcd for $C_{20}H_{34}Cl_4N_4$: C, 50.86; H, 7.26; N, 11.86%. Found: C, 50.72; H, 7.38; N, 12.16%. ^{1}H NMR (300.13 MHz, dmso-d_6, 298.2 K): δ 9.53 (br s, 2H), δ 8.62 (dd, $^3J_{HH}$ = 5.2 Hz, $^4J_{HH}$ = 1.6 Hz, 2H), δ 7.88 (dt, $^3J_{HH}$ = 7.8 Hz, $^4J_{HH}$ = 1.6 Hz, 2H), δ 7.60 (d, $^3J_{HH}$ = 7.9 Hz, 2H), δ 7.42 (dd, $^3J_{HH}$ = 5.2 Hz, $^3J_{HH}$ = 7.8 Hz, 2H), δ 4.26 (s, 4H), δ 2.91 (t, $^3J_{HH}$ = 7.7 Hz, 4H), δ 1.69 (m, 4H), δ 1.26 (m, 8H). ^{13}C NMR (75.48 MHz, dmso-d_6, 298.2 K): δ 152.10, 149.03, 137.23, 123.56, 123.49, 50.21, 46.67, 28.15, 25.79, 25.07.

4*HCl: Yield: 0.855 g (1.71 mmol, M = 500.38 g/mol, 34%). Anal. Calcd for $C_{22}H_{36}Cl_2N_4$: C, 52.81; H, 7.65; N, 12.20%. Found: C, 52.92; H, 7.59; N, 12.40%. ^{1}H NMR (300.13 MHz, dmso-d_6, 298.2 K): δ 9.90 (br s, 2H), δ 8.77 (dd, $^3J_{HH}$ = 5.1 Hz, $^4J_{HH}$ = 1.2 Hz, 2H), δ 8.21 (dt, $^3J_{HH}$ = 7.9 Hz, $^4J_{HH}$ = 1.2 Hz, 2H), δ 7.98 (d, $^3J_{HH}$ = 7.9 Hz, 2H), δ 7.70 (dd, $^3J_{HH}$ = 5.1 Hz, $^3J_{HH}$ = 7.9 Hz, 2H), δ 4.41 (s, 4H), δ 2.93 (t, $^3J_{HH}$ = 7.7 Hz, 4H), δ 1.69 (m, 4H), δ 1.25 (m, 12H). ^{13}C NMR (75.48 MHz, dmso-d_6, 298.2 K): δ 149.86, 146.07, 141.00, 125.63, 125.10, 48.41, 46.88, 28.59, 28.42, 25.91, 25.18.

Synthesis of the (*N*,*N*)-Complex System and the Mononuclear Reference Complex. [Pt_2(N^1,N^4-bis(2-pyridylmethyl)-1,4-butanediamine)Cl_4] (**5**), [Pt_2(N^1,N^6-bis(2-pyridylmethyl)-1,6-hexanediamine)Cl_4] (**6**), [Pt_2(N^1,N^8-bis(2-pyridylmethyl)-1,8-octanediamine)Cl_4] (**7**), [Pt_2(N^1,N^{10}-bis(2-pyridylmethyl)-1,10-decanediamine)Cl_4] (**8**), and [Pt(2-aminomethylpyridine)Cl_2] (**9**) were synthesized following the general procedure of Hofmann et al.[22] To a solution of 200 mg (0.48 mmol) potassium tetrachloroplatinate(II) in 50 mL 0.01 M HCl, a solution of 0.24 mmol of the corresponding ligand (0.48 mmol of 2-aminomethylpyridine) in 50 mL 0.01 M HCl was added. The solution was stirred under reflux for at least 12 h. After cooling to room temperature, the resulting precipitate was filtered off, washed carefully with water, ethanol, and diethyl ether, and dried under vacuum. All of the complexes were obtained as light-yellow powder. During complexation the NHR_2−nitrogen donor atom becomes a stereogenic center, four configurations, viz. *R*,*R*; *S*,*S*; *R*,*S*; and *S*,*R* are possible. We were not able to isolate the single diastereomers due to rapid H−exchange (mass spectrometric measurements) and consequently used a mixture of the generated species in all measurements.

5: Yield: 167 mg (0.21 mmol, M = 802.35 g/mol, 87%). Anal. Calcd for $C_{16}H_{22}Cl_4N_4Pt_2$: C, 23.95; H, 2.76; N, 6.98%. Found: C, 24.05; H, 2.71; N, 6.88%. ^{1}H NMR (300.13 MHz, dmso-d_6, 298.2 K): δ 9.03 (d, $^3J_{HH}$ = 5.3 Hz, 2H), δ 8.14 (t, $^3J_{HH}$ = 7.6 Hz, 2H), δ 7.67 (d, $^3J_{HH}$ = 7.6 Hz, 2H), δ 7.49 (dd, $^3J_{HH}$ = 5.3 Hz, $^3J_{HH}$ = 7.6 Hz, 2H), δ 7.12 (br s, N−H, 2H), δ 4.33 (d, AB spin system, $^2J_{HH}$ = 16.4 Hz, 2H), δ 4.11 (d, AB spin system, $^2J_{HH}$ = 16.4 Hz, 2H), δ 2.70 (m, 4H), δ 1.73 (m, 4H). MS-FAB (NBA, 70 eV) 766 $[M-Cl]^+$.

6: Yield: 189 mg (0.23 mmol, M = 830.41 g/mol, 95%). Anal. Calcd for $C_{18}H_{26}Cl_4N_4Pt_2$: C, 26.03; H, 3.16; N, 6.75%. Found: C, 25.95; H, 3.19; N, 6.84%. ^{1}H NMR (300.13 MHz, dmso-d_6, 298.2 K): δ 9.04 (d, $^3J_{HH}$ = 5.6 Hz, 2H), δ 8.15 (t, $^3J_{HH}$ = 7.7 Hz, 2H), δ 7.65 (d, $^3J_{HH}$ = 7.7 Hz, 2H), δ 7.50 (dd, $^3J_{HH}$ = 5.6 Hz, $^3J_{HH}$ = 7.7 Hz, 2H), δ 7.05 (br s, N−H, 2H), δ 4.32 (d, AB spin system, $^2J_{HH}$ = 16.3 Hz, 2H), δ 4.09 (d, AB spin system, $^2J_{HH}$ = 16.3 Hz, 2H), δ 2.98 (m, 4H), δ 1.45 (m, 4H), δ 1.22 (m, 4H). MS-FAB (NBA, 70 eV) 796 $[M-Cl]^+$.

7: Yield: 171 mg (0.20 mmol, M = 858.46 g/mol, 83%). Anal. Calcd for $C_{20}H_{30}Cl_4N_4Pt_2$: C, 27.98; H, 3.52; N, 6.53%. Found: C, 28.15; H, 3.50; N, 6.40%. ^{1}H NMR (300.13 MHz, dmso-d_6, 298.2 K): δ 9.03 (d, $^3J_{HH}$ = 5.1 Hz, 2H), δ 8.15 (t, $^3J_{HH}$ = 7.4 Hz, 2H), δ 7.67 (d, $^3J_{HH}$ = 7.4 Hz, 2H), δ 7.50 (dd, $^3J_{HH}$ = 5.1 Hz, $^3J_{HH}$ = 7.4 Hz, 2H), δ 7.06 (br s, N−H, 2H), δ 4.33 (d, $^2J_{HH}$ = 16.5 Hz, 2H), δ 4.09 (d, AB spin system, $^2J_{HH}$ = 16.5 Hz, 2H), δ 2.71 (m, 4H), δ 1.65 (m, 4H), δ 1.19(m, 8H). MS-FAB (NBA, 70 eV) 822 $[M-Cl]^+$.

8: Yield: 179 mg (0.20 mmol, M = 886.51 g/mol, 84%). Anal. Calcd for $C_{22}H_{34}Cl_4N_4Pt_2$: C, 29.81; H, 3.87; N, 6.32%. Found: C, 30.01; H, 3.85; N, 6.27%. ^{1}H NMR (300.13 MHz, dmso-d_6, 298.2 K): δ 9.03 (d, $^3J_{HH}$ = 5.4 Hz, 2H), δ 8.15 (t, $^3J_{HH}$ = 7.8 Hz, 2H), δ 7.68 (d, $^3J_{HH}$ = 7.8 Hz, 2H), δ 7.50 (dd, $^3J_{HH}$ = 5.4 Hz, $^3J_{HH}$ = 7.8 Hz, 2H), δ 7.05 (br s, N−H, 2H), δ 4.33 (d, AB spin system, $^2J_{HH}$ = 16.5 Hz, 2H), δ 4.10

(d, AB spin system, $^2J_{HH}$ = 16.5 Hz, 2H), δ 2.72 (m, 4H), δ 1.75 (m, 2H), δ 1.50 (m, 2H), δ 1.19 (m, 12H). MS-FAB (NBA, 70 eV) 885 $[M]^+$, 851 $[M-Cl]^+$.

9: Yield: 146 mg (0.39 mmol, M = 374.13 g/mol, 81%). Anal. Calcd for $C_6H_8Cl_2N_2Pt$: C, 19.26; H, 2.16; N, 7.49%. Found: C, 19.46; H, 2.10; N, 7.19%. ^{1}H NMR (300.13 MHz, dmso-d_6, 298.2K): δ 9.03 (d, $^3J_{HH}$ = 5.4 Hz, 1H), δ 8.10 (t, $^3J_{HH}$ = 7.8 Hz, 1H), δ 7.68 (d, $^3J_{HH}$ = 7.8 Hz, 1H), δ 7.46 (dd, $^3J_{HH}$ = 5.4 Hz, $^3J_{HH}$ = 7.8 Hz, 1H), δ 6.82 (br s, NH_2, 2H), δ 4.41 (t, AB spin system, $^2J_{HH}$ = 16.5 Hz, 1H), δ 4.07 (t, AB spin system, $^2J_{HH}$ = 16.5 Hz, 1H).

Preparation of the Complex Solutions.[22]. The desired solutions of the aqua complexes were prepared by suspending a defined amount of the corresponding chloro complexes **5**−**9** in 0.001 M triflic acid and adding a stoichiometric excess of silver triflate (4.1 eq for the dinuclear system and 2.1 eq in case of the mononuclear complex) with respect to the chloro ligands. The mixture was then stirred in the dark for at least 2 days at 45 °C, which led to the formation of silver chloride. The precipitated silver chloride was filtered off, and the pH of the resulting solution was increased to 11 by addition of small amounts of 0.1 M NaOH solution. This led to the formation of brown silver oxide (from the excess silver triflate), which was then removed with a Millipore filter, and the pH of the remaining solution was adjusted to pH 2 with triflic acid to give the desired complex concentration of 0.2 mM. For all kinetic investigations, the pH of the solution was kept at 2 and the ionic strength was adjusted to 0.01 M with triflic acid.

Instrumentation and Measurement. NMR spectroscopy (Bruker Avance DPX 300) and a Carlo Erba Elemental Analyzer 1106 were used for ligand and complex characterization and chemical analysis, respectively. Mass spectrometric measurements were performed on an UHR-TOF Bruker Daltonik (Bremen, Germany) maXis, an ESI-TOF mass spectrometer capable of a resolution of at least 40 000 fwhm used by the group of Prof. Ivana Ivanović-Burmazović at the University of Erlangen-Nürnberg. A Varian Cary 1G spectrophotometer equipped with a thermostatted cell holder was used to record UV−vis spectra for the determination of the pK_a values of the aqua complexes. Kinetic measurements on fast reactions were performed on an Applied Photophysics SX 18MV stopped-flow instrument and for the study of slow reactions a Shimadzu UV-2010PC spectrophotometer with a thermoelectrically controlled cell holder was used. Experiments at elevated pressure were performed on a laboratory-made high-pressure stopped-flow instrument for fast reactions.[23] The temperature of the instruments was controlled throughout all kinetic experiments to an accuracy of ±0.1 °C. The values of the reported pseudofirst-order rate constants are the average of at least four kinetic measurements.

Mass Spectrometric Measurements. After complexation, the NHR_2−nitrogen donor atom becomes a stereogenic center. Consequently four possible configurations, viz. *R,R*; *S,S*; *R,S*; and *S,R* can be present in solution. Attempts to isolate the different species were not successful. The NHR_2−nitrogen atom is formally positively charged and we therefore suggest that the hydrogen atom bound to nitrogen can easily exchange such that it will be impossible to obtain pure isomers. To support this presumption, we decided to perform H/D−exchange experiments. Because of the low solubility of the complexes, NMR techniques gave unsatisfying results because the concentration of the complex in solution is too low for such experiments. Hence, we repeated the H/D−exchange measurements and monitored the generated species using mass spectrometry. Detection was in the positive-ion mode and the source voltage was 3.4 kV. The flow rate was 500 μL/h. The drying gas (N_2) to aid solvent removal was kept at 180 °C. The instrument was calibrated prior to every experiment via direct infusion of the Agilent ESI-TOF low concentration tuning mixture, which provided a m/z range of singly charged peaks up to 2700 Da in both ion modes. A big advantage using this technique is that it only requires low concentrations of about 10^{-7} molar. The tetrachloro species of the

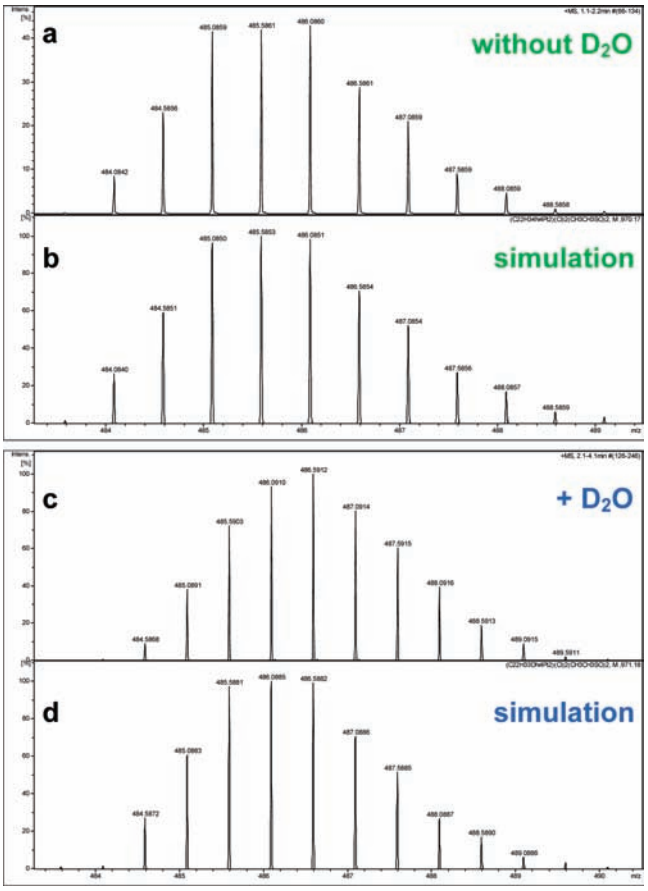

Figure 3. Isotopic patterns of the peak around m/z = 486, which belongs to the **10NNpy** complex that includes two chloride and two dmso ligands, (a) without D_2O, (b) simulation of the pattern without D_2O, (c) after addition (12 h) of D_2O, (d) simulation of the pattern including one deuterium atom.

10NNpy complex (**8**) was dissolved in 2 mL dmso and a mass spectrum of the solution was recorded. We observed no tetrachloro species in the spectra, which is not surprising because the tetrachloro complex is neutral and therefore a poorly soluble species. The major peak at m/z 929.1273 could be assigned to the complex with 3 chloride ligands, one dmso ligand, and consequently 1+ charged. Another peak with high intensity was found at m/z 486.0860 with a molecular weight of 972.1720, 2+ charged and including 2 chloride and 2 dmso ligands (also Figure S1 of the Supporting Information). After analyzing the existing peaks, a few drops of D_2O were added to the dmso solution and stirred. After 10 min, no clear changes could be observed. Upon stirring the solution overnight, the major peak of the spectra appeared at m/z 486.5912 (a molecular weight of 973.1824), which could be assigned to the deuterated NDR_2 nitrogen donor (Figure S2 of the Supporting Information).

Compared to the isotopic pattern in the absence of D_2O (top of Figure 3), a clear shift of 0.5 m/z due to the exchange of H by D can be seen (bottom of Figure 3). Furthermore, it shows that on a longer time scale the complex loses one chloride and ends up in a 2+ charged species with 2 chloride and 2 dmso ligands. The clear evidence for H/D − exchange is of significant importance because it explains why in solution a mixture of all possible configurations is always observed and that it is impossible to isolate one of them in a pure form.

Computational Details. As a test case, **4NNpy** and the corresponding deprotonated species were fully optimized using the B3LYP hybrid density functional[24] and the LANL2DZ basis set.[25] All structures

dx.doi.org/10.1021/ic201151h |*Inorg. Chem.* 2011, 50, 8984–8996

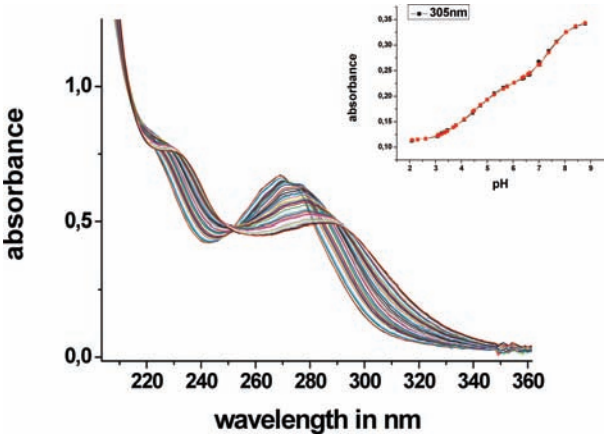

Figure 4. UV−vis spectra recorded for 0.05 mM **4NNpy** in the pH range 2−9 at 25 °C. Insert: Plot of absorbance vs pH at 305 nm.

were characterized as minima by computation of vibrational frequencies. Following the procedure of Gilson and Durrant,[26] the pK_a values were derived by PCM[27] single point calculations. **4NNpy** and all other systems were further optimized and characterized as minima by applying the pure density functional BP86[28] together with the LACVP* basis set[25,29] and the density fitting approximation.[30] The *Gaussian 03* suite of programs was used throughout.[31]

RESULTS AND DISCUSSION

pK_a Determination of the Tetraaqua Complexes. To obtain information on the acidity of the coordinated water ligands and therefore, on the reactivity of all of the aqua complexes, their pK_a values were determined. For this reason, a spectrophotometric pH titration with NaOH as base in the pH range of 2−9 was performed. The spectrophotometric pK_a determination was done using a Hellma optical cell for flow-through measurements attached to a peristaltic pump. Thereby, it was important to keep the concentration of the complex solution constant to avoid absorbance corrections due to dilution. This can be achieved using a large volume of 100 mL complex solution during the titration. Starting at pH 2, the pH was increased by addition of small portions of solid NaOH to the solution until a pH of 3 was reached. For further increase in pH, a series of NaOH solutions with different concentrations were used. The consecutive pH changes were obtained by dipping a needle into these NaOH solutions and then in the complex solution. After each addition of base, samples of 500 μL were taken from the complex solution and the pH was measured at 25 °C using an InLab Semi-Micro pH electrode. This electrode was calibrated using standard buffer solutions at pH 4, 7, and 10, purchased from Fisher Scientific. Afterward, the samples were discarded because of a possible chloride ion contamination coming from the pH electrode. Each pK_a titration was performed at least two times and an average of both values was taken. The pH dependence of the aqua complex was monitored by UV−vis spectroscopy. Figure 4 (also Figures S3−S6 of the Supporting Information) shows a typical example (**4NNpy**) of a titration with its spectral changes recorded as a function of pH. The overall process can be presented by Scheme 1. The spectral data were analyzed using the *Specfit Global Analysis* software. Eigen vector analysis with *Specfit* indicates that there are five colored species for each dinuclear system and three colored species for the mononuclear reference

Scheme 1. Proposed Stepwise Deprotonation for the pH Dependence of the Dinuclear Systems

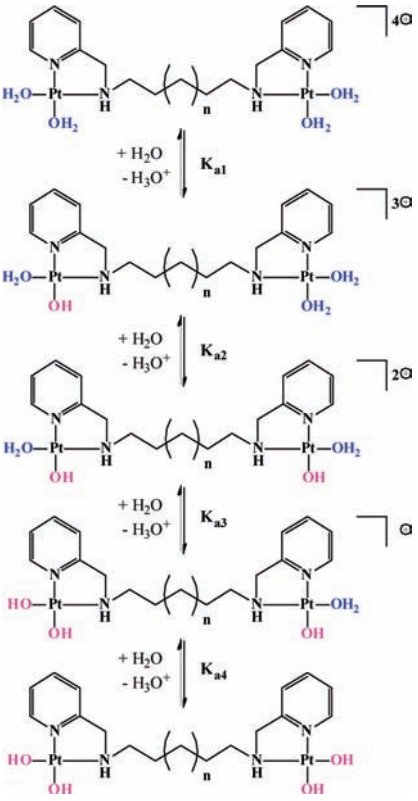

complex present in solution as a function of pH with the acid dissociation constants K_{a1}, K_{a2}, K_{a3}, and K_{a4} for the dinuclear system, and K_{a1} and K_{a2} for the mononuclear complex, respectively. The obtained data for the coordinated water ligands are summarized in Table 1.

Because the complex system includes two different types of donors, viz. an aromatic pyridine unit and a sp^3-hybridized secondary amine (NHR_2) unit, it is difficult to distinguish which water ligand is deprotonated first, that is the one trans to pyridine or the one trans to NHR_2. Because of the fact that the determined pK_a values for the dinuclear systems were found to be rather low, a closer look at the mononuclear reference complex **monoNNpy** was taken. Repeated measurements showed pK_{a1} = 4.77 and pK_{a2} = 6.56 for the first and second deprotonation steps, respectively. Compared to the data for $[Pt(en)(OH_2)_2]^{2+}$ (pK_{a1} = 5.8, pK_{a2} = 7.6, en = ethylenediamine)[32] and [*cis*-$Pt(NH_3)_2(OH_2)_2]^{2+}$ (pK_{a1} = 5.37, pK_{a2} = 7.21),[33] which represents typical values for sp^3-hybridized amines,[34] the lower pK_a values indicate that, by the addition of an in-plane pyridine unit to the chelate system, the electron density on the Pt(II) center and the hydroxo ligand is stabilized by the electron withdrawing ability of the π−accepting pyridine ring, which leads to lower pK_a values compared to complexes without π−acceptor abilities.[35] The difference between the first and second deprotonation steps is larger than reported in earlier work[36] and indicates that there is in fact a preferred first deprotonation position on each Pt(II) center.

We propose that the first deprotonation step occurs trans to the pyridine unit as shown in Scheme 1. The secondary amine NHR_2 has a stronger σ−donor ability than the pyridine unit.

dx.doi.org/10.1021/ic201151h |*Inorg. Chem.* 2011, 50, 8984–8996

Table 1. Summary of pK_a Values Obtained for the Stepwise Deprotonation of Platinum-Bound Water

	4NNpy	6NNpy	8NNpy	10NNpy		monoNNpy
pK_{a1}	3.58 ± 0.01	3.62 ± 0.03	3.64 ± 0.02	3.77 ± 0.07	pK_{a1}	4.77 ± 0.02
pK_{a2}	4.50 ± 0.07	4.41 ± 0.05	4.23 ± 0.02	4.20 ± 0.01		
pK_{a3}	5.65 ± 0.09	5.96 ± 0.03	6.22 ± 0.02	6.45 ± 0.02	pK_{a2}	6.56 ± 0.04
pK_{a4}	7.87 ± 0.07	7.84 ± 0.04	7.81 ± 0.03	7.56 ± 0.04		

Therefore, the water ligand trans to NHR_2 is labilized more due to the strong trans influence. As a consequence, this water ligand is weaker bound and has a higher pK_a value than the water trans to the pyridine nitrogen. Furthermore, a hydroxo ligand positioned trans to the π−accepting pyridine ligand is stabilized and favors the deprotonation at this site. These suggestions are valid for the **monoNNpy** reference complex and the dinuclear **NNpy** complexes studied in this work.

The results shown in Table 1 indicate a correlation between the pK_a values and the aliphatic chain length of the complexes. The pK_{a1} value (3.58−3.77) is always lower than that for the mononuclear reference complex (4.77). The slight increase in the pK_{a1} values in the order **4NNpy** < **6NNpy** < **8NNpy** < **10NNpy** arises from lengthening the aliphatic chain and the decrease in the localized charge on the Pt center with decreasing communication between the two Pt centers. We suggest that this small increase (only 0.2 pK_a units from the shortest to the longest chain) is a result of charge effects and not of σ−donation by the aliphatic chains. In addition, the difference between pK_{a1} and pK_{a2}, as well as the difference between pK_{a3} and pK_{a4}, become smaller with increasing chain length. This corroborates earlier work performed in our group.[15,37] The first and second deprotonation steps occur trans to the pyridine unit on each Pt center. In the dinuclear Pt(II) complexes of shorter distance between the Pt centers, the charges on each Pt center add up to an overall charge of 4+. This leads to more electrophilic Pt centers and therefore to lower pK_a values for the coordinated water ligands compared to the 2+ charged mononuclear complex. As mentioned above, the effect of charge addition decreases as the distance between the Pt centers becomes longer. This effect again explains why with increasing chain length the difference between pK_{a1} and pK_{a2} becomes smaller. The third deprotonation step takes place trans to the NHR_2 unit. The overall charge of the complex is now 2+, which results in higher pK_a values compared to those for the first two steps. At this point the chain length influences the pK_{a3} values. With increasing chain length the NHR_2 unit receives more electron density and therefore produces a stronger σ−donor effect on the trans localized water ligand. As a consequence, the water ligands become more labilized and the pK_{a3} values increase in the order **4NNpy** < **6NNpy** < **8NNpy** < **10NNpy** (nearly 1 pK unit from the shortest to the longest chain length). The final deprotonation step shows the highest pK_{a4} values due to the overall charge of 1+. The values are almost independent of the aliphatic chain length, which is presumably a result of the three hydroxo ligands that overrule the charge density on the Pt centers.

Farrell and co-workers also determined pK_a values for polynuclear Pt(II) complexes, where the relevant Pt centers are far away from each other, and only one pK_a value for two water molecules was obtained.[38] Thus, we expect for the complexes studied in this work that on exceeding a specific chain length, it will not be possible to differentiate between the two metal centers in terms of their electrophilicity and acidity anymore. At a certain chain length the dinuclear complexes will behave like two equal mononuclear Pt(II) complexes and show two pK_a values for the two water ligands bound to the Pt center.

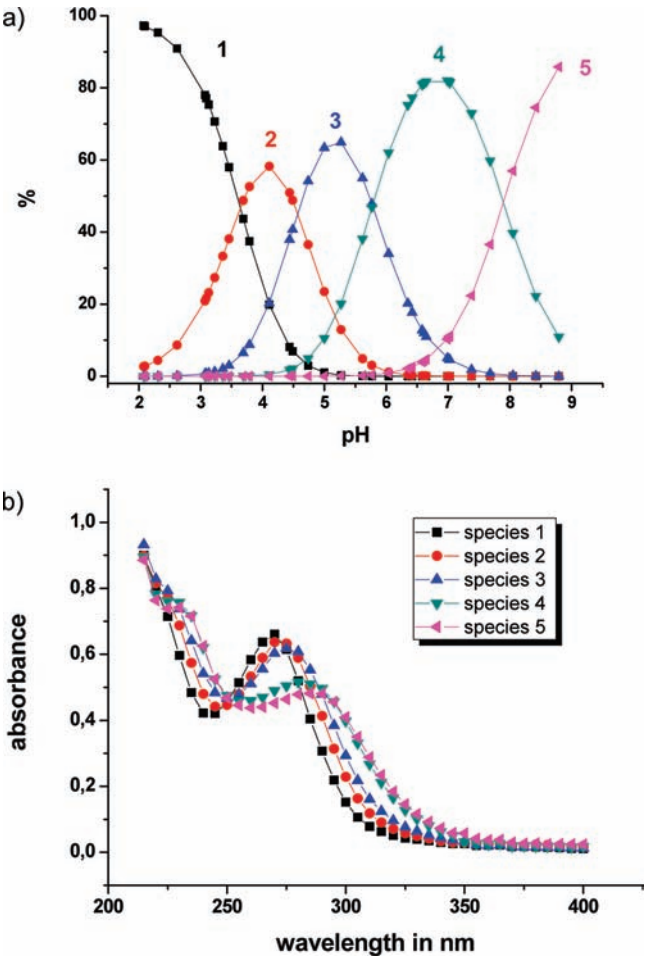

Figure 5. (a) Distribution of the different species 1−5 present in solution for 0.05 mM **4NNpy** complex at different pH with: species 1 − $[Pt_2(OH_2)_4]^{4+}$, species 2 − $[Pt_2(OH_2)_3(OH)]^{3+}$, species 3 − $[Pt_2(OH_2)_2(OH)_2]^{2+}$, species 4 − $[Pt_2(OH_2)(OH)_3]^{+}$, species 5 − $[Pt_2(OH)_4]$; (b) calculated absorbance traces for each species 1−5 for the **4NNpy** complex.

Part a of Figure 5 shows a typical example of the distribution of the five species consecutively generated in solution as a function of pH for a 0.05 mM solution of **4NNpy**. On the basis of such diagrams, it is possible to calculate the percentage distribution at a specific pH. For instance, at pH 2 there are 98% tetraaqua and 2% triaqua-monohydroxo species present in solution, whereas at pH 7.4 (interesting for physiological conditions) already 50% monoaqua-trihydroxo, 48% tetrahydroxo only 2% diaqua-dihydroxo species are generated in solution. Figure 5 shows that, with increasing pH, the minimum and maximum of each species are

dx.doi.org/10.1021/ic201151h |*Inorg. Chem.* 2011, 50, 8984–8996

Scheme 2. Proposed Substitution Reactions with a Nucleophile (Nu = Thiourea)

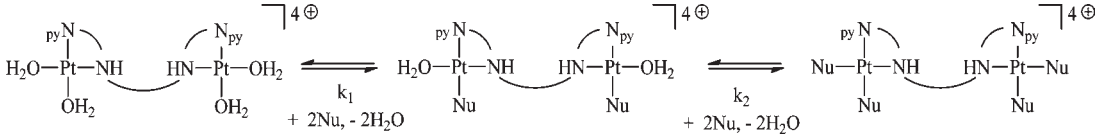

shifted toward higher wavelengths and a new band is formed at about 225 nm. It is known from the literature that μ-hydroxo-bridged dimers, trimers, and tetramers can be accumulated in solution at higher pH.[39] To prevent the formation of such species, the pH titrations were carried out at low concentrations of 0.05 mmol/L. During the titrations, no evidence for polymer formation could be found.

To provide further evidence that the first deprotonation step takes place trans to the pyridine unit, additional quantum chemical calculations were performed. For this purpose, the simple but promising approach of Gilson and Durrant[26] based on B3LYP(PCM)/LANL2DZ energy calculations[24−27] was used to derive pK_a data for the mononuclear reference complex as well as for the dinuclear systems (Table S1 of the Supporting Information). The calculated data clearly verify that the first two successive deprotonation steps do not occur at the same Pt center, as expected. In contrast, we were not able to distinguish between which coordinated water ligand deprotonated first. The stability differences in the two possible isomers, for example in **monoNNpy**, is 0.2 kcal/mol.[36] This energy difference leads in the Gilson and Durrant method to a pK_a difference of 0.1 units, which is beyond the accuracy of the data. Nevertheless, the calculations showed that a small change in energy (<1%) provokes an immense change in the pK_a value. Therefore, we learned that this method is too simple to be used for more complicated systems and that the calculations neither confirm nor refute our conclusions.

Kinetic Measurements with Thiourea. The substitution behavior of a series of tetraaqua complexes (Figure 2) with thiourea (tu) as a strong nucleophile was studied because of the biological role sulfur-containing molecules play in side reactions in blood and cells.[2] It is well-known that sulfur-containing compounds are used as protective and rescue agents to prevent side effects.[40] Furthermore, thiourea is an adequate nucleophile to study ligand substitution reactions in coordination chemistry because of its good solubility, neutral character, and high nucleophilicity. For the kinetic measurements, at least a 50-fold excess of thiourea relative to the complex concentration was used to guarantee pseudofirst-order conditions for the consecutive substitution reactions. Because it is known that triflate anions do not coordinate to Pt(II) metal centers,[41] 0.01 M triflic acid (pH 2) was used as solvent for all measurements, which leads to an ionic strength of 0.01 M. Furthermore, the pH of 2 was selected to maximize the concentration of the tetraaqua complex and to prevent the formation of hydroxo species, which are known to be inert against further substitution.[42,43] Because of the stereogenic nitrogen donor atom of the NHR_2 unit, and the possibility of hydrogen exchange at this nitrogen atom (mass spectrometric measurements), there is always a mixture of diastereomers and enantiomers present in solution. During the kinetic experiments, no evidence was observed for the different species in solution. We suggest that the configuration at the NHR_2 unit does not affect the rate of the substitution reactions because thiourea is a

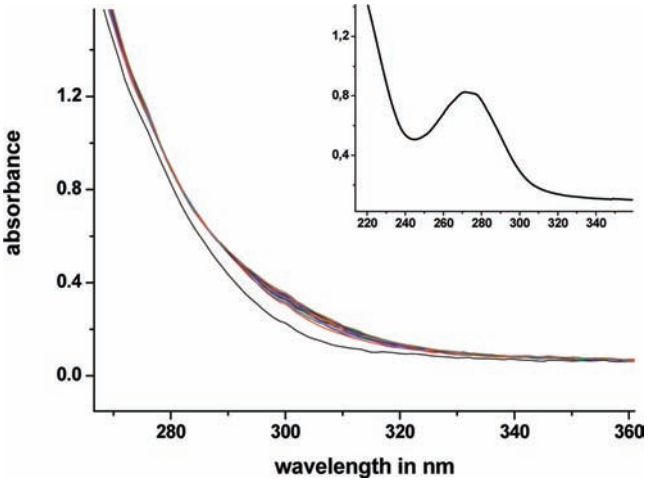

Figure 6. UV−vis spectra recorded for the reaction of 0.1 mM **10NNpy** with 5 mM thiourea at 25 °C and pH 2. Insert: absorbance of 0.2 mM **10NNpy** in the absence of thiourea.

steric nondemanding nucleophile and also the hydrogen atom that can switch its position is small and sterically nondemanding.

On using thiourea as a neutral nucleophile, the charge on the complex remains constant during the substitution steps. Because of the C_2−symmetry of the complexes, two water ligands are equivalent and substituted simultaneously, such that two reaction steps are expected. Scheme 2 shows the substitution reaction, and eqs 1 and 2 the corresponding rate laws:

$$k_{obs1} = k_1[Nu] + k_{-1} \approx k_1[Nu]\ Nu = thiourea \quad (1)$$

$$k_{obs2} = k_2[Nu] + k_{-2} \approx k_2[Nu]\ Nu = thiourea \quad (2)$$

By way of example, the absorbance changes observed during the reaction of 0.1 mM **10NNpy** with 5 mM thiourea are presented in Figure 6 (also Figures S7−S9 of the Supporting Information). The spectra show a large change in absorbance that results in an isosbestic point around 288 nm, which represents the first fast substitution step, followed by a steady increase in absorbance until the end of the reaction is reached. On the basis of the information obtained from these spectra, the wavelength 288 nm was selected to follow the first fast reaction and the wavelength 310 nm was selected to observe the second slower substitution step.

The time-dependent spectra observed for the reactions of all complexes match perfectly to a single exponential fit at 288 nm (Figures S10−S13 of the Supporting Information). At this selected wavelength, the second substitution step does not have to be taken into account. However, at a wavelength of 310 nm, the data show a double exponential behavior due to the interference of

dx.doi.org/10.1021/ic201151h |*Inorg. Chem.* 2011, 50, 8984–8996

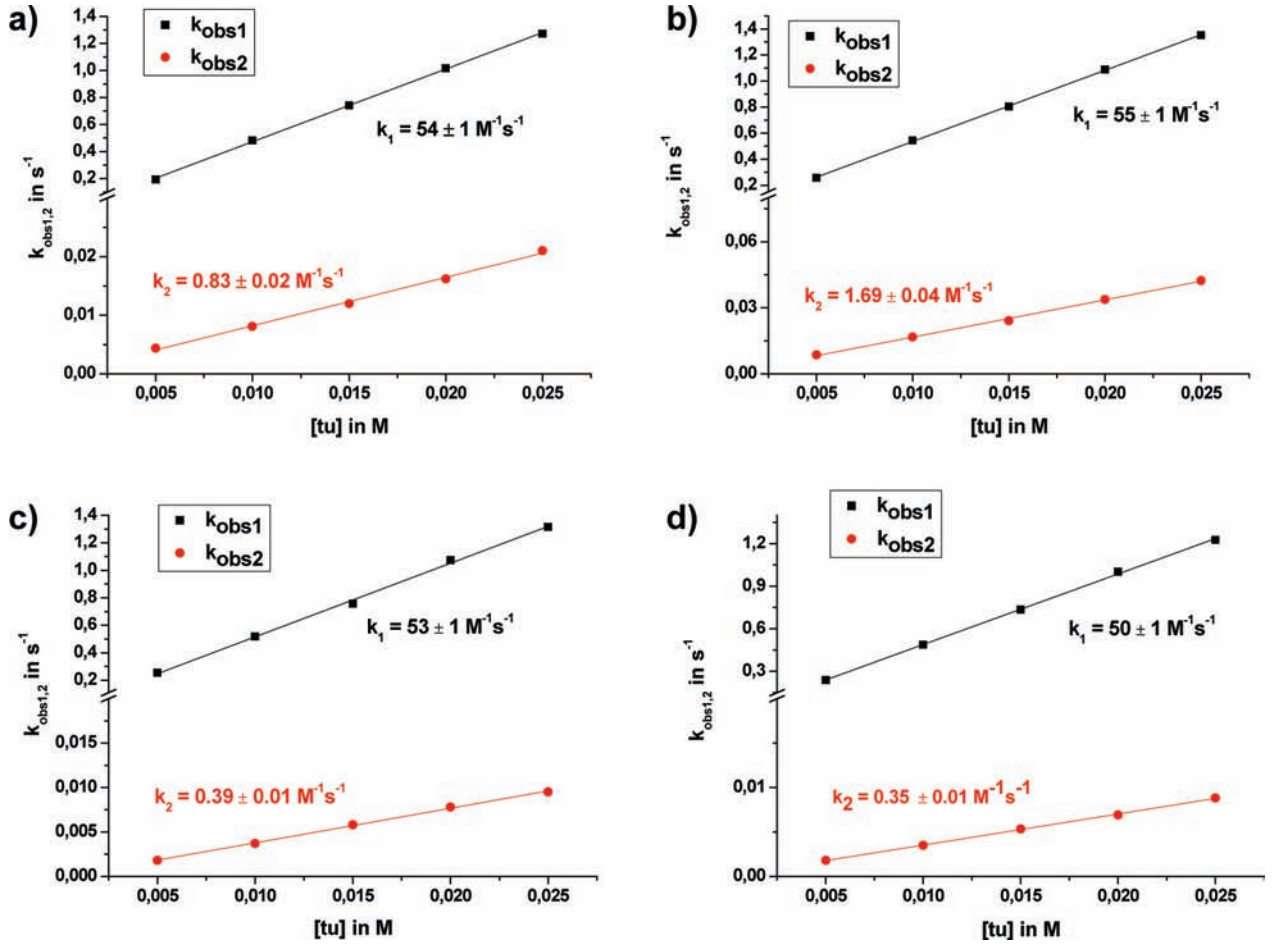

Figure 7. a) Plots of k_{obs1} and k_{obs2} vs thiourea concentration for the reaction with 0.1 mM **4NNpy** in 0.01 M triflic acid (pH 2, I = 0.01 M) at 25 °C. b) Plots of k_{obs1} and k_{obs2} vs thiourea concentration for the reaction with 0.1 mM **6NNpy** in 0.01 M triflic acid (pH 2, I = 0.01 M) at 25 °C. c) Plots of k_{obs1} and k_{obs2} vs thiourea concentration for the reaction with 0.1 mM **8NNpy** in 0.01 M triflic acid (pH 2, I = 0.01 M) at 25 °C. d) Plots of k_{obs1} and k_{obs2} vs thiourea concentration for the reaction with 0.1 mM **10NNpy** in 0.01 M triflic acid (pH 2, I = 0.01 M) at 25 °C.

Table 2. Summary of the Rate Constants for the Displacement of Coordinated Water by Thiourea at 25 °C and pH 2 (0.01 M Triflic Acid)

	monoNNpy[a]	4NNpy	6NNpy	8NNpy	10NNpy
k_1 in M^{-1} s^{-1} at 288 nm	233 ± 5	55.2 ± 0.4	53.9 ± 0.6	53 ± 1	52.2 ± 0.3
k_2 in M^{-1} s^{-1} at 310 nm	38 ± 1	1.69 ± 0.04	0.83 ± 0.02	0.39 ± 0.01	0.35 ± 0.01
$\Delta H^{\#}_1$ in kJ mol^{-1}	52 ± 3	43 ± 1	43 ± 1	42 ± 1	44 ± 2
$\Delta S^{\#}_1$ in J mol^{-1} K^{-1}	−28 ± 9	−68 ± 4	−69 ± 4	−69 ± 3	−66 ± 6
$\Delta H^{\#}_2$ in kJ mol^{-1}	35 ± 1	49 ± 2	45 ± 1	43 ± 1	37 ± 1
$\Delta S^{\#}_2$ in J mol^{-1} K^{-1}	−95 ± 3	−78 ± 6	−92 ± 4	−111 ± 4	−128 ± 3
$\Delta V^{\#}_1$ in cm^3 mol^{-1}	−6.27 ± 0.03	−7.4 ± 0.4	−7.7 ± 0.3	−8.0 ± 0.1	−7.8 ± 0.1
$\Delta V^{\#}_2$ in cm^3 mol^{-1}		−9.9 ± 0.4	−10.8 ± 0.3	−11.7 ± 0.9	−12.6 ± 0.2

[a] Ref 36.

the first reaction step (Figures S14−S17 of the Supporting Information). The determined pseudofirst-order rate constants, k_{obs1} and k_{obs2}, were plotted against the thiourea concentration and resulted in a linear dependence with no meaningful intercept. This indicates that the reverse reaction with water is too slow and can be neglected. Figure 7 reports the nucleophile concentration dependences for the two rate constants k_{obs1} and k_{obs2} for all the dinuclear complex systems studied (also Tables S2−S3 of the Supporting Information).

Table 2 summarizes the obtained rate constants for the first and second reaction steps. It is noticed that the values for the first substitution rate constant k_1 are almost the same (~53 M^{-1} s^{-1}) and apparently not influenced by the varying chain length. Only the second substitution step k_2 shows a clear dependence on the chain length in the order **4NNpy** (1.69 M^{-1} s^{-1}) > **6NNpy** (0.89 M^{-1} s^{-1}) > **8NNpy** (0.39 M^{-1} s^{-1}) > **10NNpy** (0.35 M^{-1} s^{-1}). As a result of the reported pK_a values, we found the more labile water molecule to be trans to the NHR_2 unit,

dx.doi.org/10.1021/ic201151h |*Inorg. Chem.* 2011, 50, 8984–8996

Scheme 3. Visualization of the Different Coordination Spheres during Substitution of the First Water Molecule by Thiourea (L)

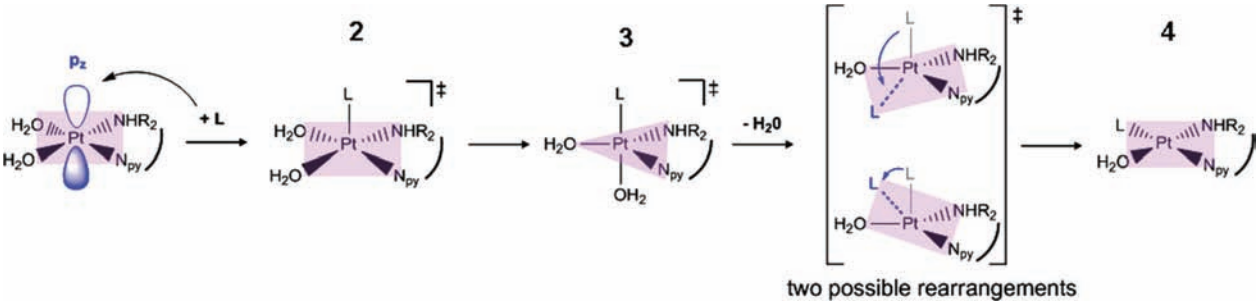

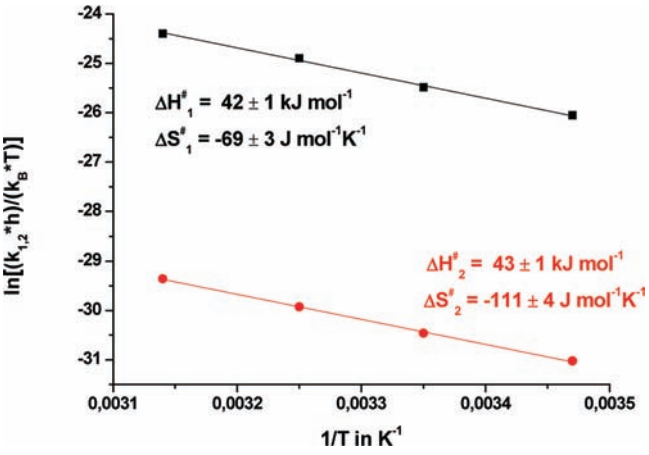

Figure 8. Eyring plots for the determination of the thermal activation parameters for the two reaction steps of 0.1 mM **8NNpy** with 15 mM thiourea at 25 °C and pH 2 (I = 0.01 M triflic acid).

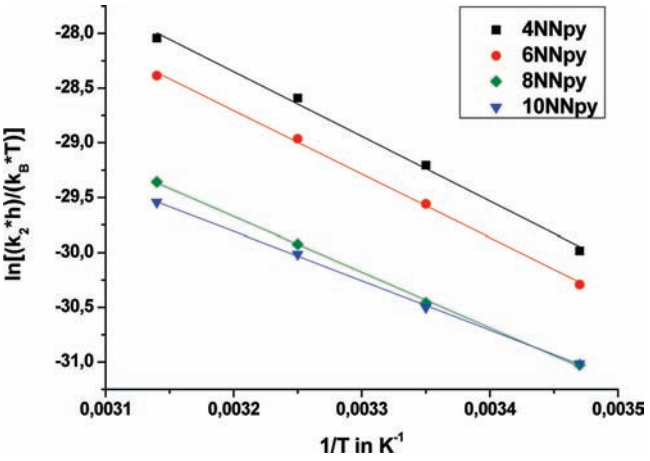

Figure 9. Eyring plots for the determination of the thermal activation parameters of k_2 for all dinuclear complexes studied with 15 mM thiourea at 25 °C and pH 2 (I = 0.01 M triflic acid).

which should be substituted first. However, the theoretical and experimental behavior shows exactly the opposite. Theoretically the first substitution step should take place trans to the NHR_2 unit and therefore should be influenced by the varying chain length, whereas the second substitution step should occur trans to the pyridine unit and be independent of the chain length.

To clarify these opposite trends, we took a closer look at the complex structure itself. It contains two completely different N-containing donor atoms, viz. a pyridine donor with its strong π−accepting ability and a secondary amine donor with σ−donor ability. These forces compete with each other in the first substitution step as shown in Scheme 3.

As known from the literature,[44] Pt(II) complexes have a square-planar coordination sphere and the entering ligand (L) interacts with the empty p_z orbital of the platinum center to first form a quadratic pyramidal transition state (**2** in Scheme 3). This reaction in general controls the rate of the overall ligand substitution process. We assume that the strong π−accepting ability of the pyridine ligand at this point overrules the σ−donor effect of the secondary amine function, such that the electrophilicity of the Pt(II) center controls the associative bond formation process. Therefore the electrophilicity of the Pt(II) center is expected to be similar for all of the complexes studied, thus independent of the chain length and its inductive effect. The next step is a rearrangement of the quadratic pyramidal transition state to a trigonal bipyramidal intermediate, where the most labile water ligand is localized trans to the incoming ligand L (**3** in Scheme 3). On the basis of the information obtained from the pK_a values, this labilized water molecule is the one previously bound trans to the NHR_2 unit and will therefore be the one to leave the coordination sphere first. The last step is the rearrangement from a trigonal pyramidal intermediate back to a square-planar ground state (**4** in Scheme 3). At this point the strong π−acceptor effect of the pyridine unit plays a crucial role because there are two possible modes of rearrangement in the transition state as shown in Scheme 3. The strong π−acceptor effect favors the displacement of the entering ligand (thiourea) trans to the pyridine rather than trans to the NHR_2 unit. Thereby the strong σ−donor property of thiourea is best compensated by the strong π−accepting ability of the pyridine ligand.

The compensation of the π−acceptor character of pyridine leads to a clear dependence of the second substitution reaction on the chain length of the dinuclear complexes. On increasing the chain length, the Pt(II) center becomes less electrophilic, which slows down the nucleophilic attack such that the rate constants for the second step k_2 follow the order **4NNpy** > **6NNpy** > **8NNpy** > **10NNpy** (Table 2). In general, the second substitution reaction occurs slower due to steric hindrance of the coordinated thiourea ligand and the lower electrophilic of the Pt(II) center following the first substitution reaction. The lack of an aliphatic chain and its effect on the second substitution step in the mononuclear complex accounts for the very close values of k_1 and k_2 as compared to that found for the dinuclear systems.[36]

dx.doi.org/10.1021/ic201151h |*Inorg. Chem.* 2011, 50, 8984–8996

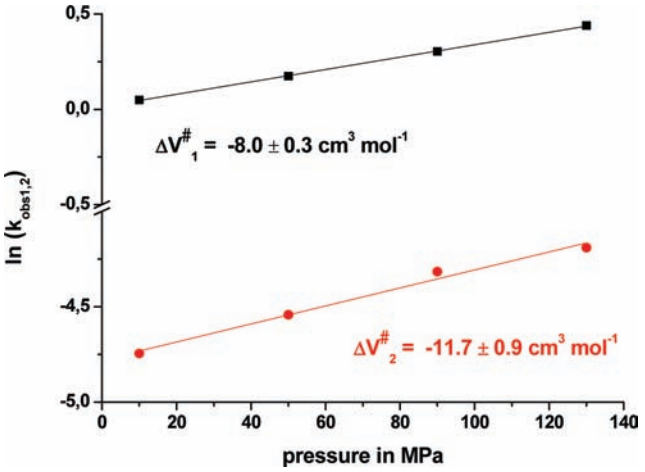

Figure 10. Plots of $\ln(k_{obs})$ vs pressure for the reaction of 0.1 mM **8NNpy** with 25 mM thiourea at 25 °C and pH 2 (I = 0.01 M triflic acid).

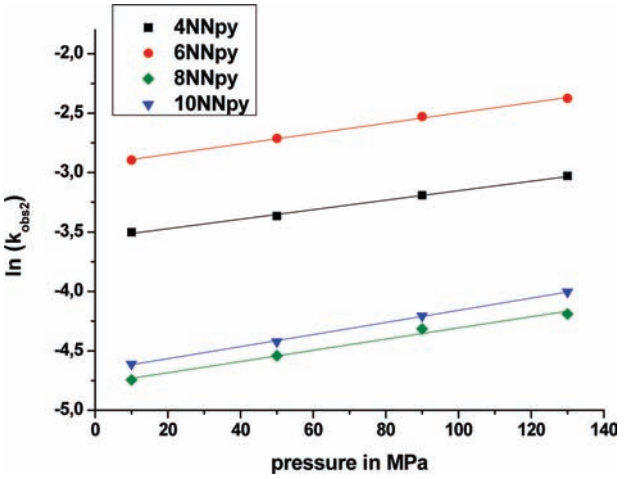

Figure 11. Plots of $\ln(k_{obs2})$ vs pressure for the second reaction step for all complexes studied with 25 mM thiourea at 25 °C and pH 2 (I = 0.01 M triflic acid).

In addition, temperature and pressure dependence studies were performed to gain more insight into the nature of the substitution mechanism from the thermal and pressure activation parameters. The thermal parameters $\Delta H^{\#}$ and $\Delta S^{\#}$ were determined by measuring the rate constants of each substitution step of each complex at a fixed thiourea concentration (15 mM) as a function of temperature as seen in Figures 8 and 9 (also Figures S18−S23 and Tables S4−S5 of the Supporting Information). The data were calculated using the Eyring equation for which the observed first-order rate constants were converted to second-order rate constants ($k = k_{obs}/[tu]$) based on eqs 1 and 2, and the results are summarized in Table 2. As expected, the activation enthalpy $\Delta H^{\#}_1$ of the first reaction step shows very similar values of about +43 kJ mol^{-1} for all studied complexes, and the activation entropies $\Delta S^{\#}_1$ have negative values of about −68 J mol^{-1} K^{-1}. However, in the case of k_2 the decrease in rate constant with increasing length of the aliphatic chain is accompanied by a decrease in $\Delta H^{\#}_2$ and a decrease in $\Delta S^{\#}_2$ (further discussion).

Furthermore, pressure dependence studies were performed by measuring the rate constants of each substitution step of each complex at a fixed thiourea concentration (25 mM) as a function of pressure as seen in Figures 10 and 11 (also Figures S24−S29 and Tables S6−S7 of the Supporting Information). The volumes of activation $\Delta V^{\#}$, calculated from the slope of plots of $\ln(k_{obs})$ versus pressure, are summarized in Table 2. Throughout the series of complexes the substitution reactions were accelerated with increasing pressure. The so-obtained activation volumes are very typical for associative substitution reactions on square-planar complexes,[45−47] where the volume decrease results from bond formation on going from the square-planar reactant state to the trigonal bipyramidal transition state. This mechanistic assignment is furthermore in agreement with significantly negative activation entropies found for both reaction steps of all dinuclear complexes (Table 2).

Table 3. Summary of the Chemical Quantum Calculations for the Mononuclear and Dinuclear Complexes

	mono NNpy	4NNpy	6NNpy	8NNpy	10NNpy
Φ (N_{py}−Pt···Pt−N_{py}) in °		121.1	123.4	123.9	121.7
Φ (N−CH_2− C_{py}y−N_{py}) in °	26.7	29.0	28.6	28.4	28.4
d Pt−N_{amine} in Å	2.05	2.08	2.07	2.07	2.07
d Pt−$O_{trans\ to\ amine}$ in Å	2.13	2.16	2.16	2.17	2.17
d Pt−N_{py} in Å	2.00	2.01	2.01	2.01	2.01
d Pt−$O_{trans\ to\ py}$ in Å	2.16	2.17	2.17	2.17	2.17
d Pt−Pt in Å		10.02	12.56	15.11	17.70
d N−$(CH_2)_n$−N in Å		6.48	9.04	11.60	14.15

Interestingly, clear trends can be observed in the reported activation parameters and determine the reactivity of the investigated dinuclear complexes. The first substitution step is independent of the length of the bridging aliphatic chain. The rate constants k_1 as well as the activation parameter $\Delta H^{\#}_1$, $\Delta S^{\#}_1$, and $\Delta V^{\#}_1$ show no significant change with increasing chain length. As mentioned before, this effect can be attributed to the strong influence of the pyridine unit in the trans position. It consists of σ- and π-contributions,[48] whereas the first can be seen in the ground state labilization[49] and the second in the transition state stabilization.[50] This effect overrules the influence of the electron donating aliphatic chain and results in similar k_1 values and activation parameters for the first substitution step. However, after coordination of the first thiourea ligand trans to the pyridine unit, this effect is compensated by the strong σ−donor effect of the thiourea ligand compared to that of the pyridine unit. The former strong Pt−$N_{pyridine}$ bond elongates and becomes weaker such that the influence of the aliphatic chain becomes more important. As mentioned before, this leads to a decrease in k_2 with increasing aliphatic chain length. Surprisingly, however, this trend is accompanied by a decrease in both the activation enthalpy and entropy (Table 2). The overall activation barrier $\Delta G^{\#}$ (= $\Delta H^{\#} - T\Delta S^{\#}$) increases slightly with increasing chain length as a result of the increasing contribution from $T\Delta S^{\#}$. For the shortest chain (**4NNpy**) the entropic contribution is approximately 30% of the overall activation barrier, whereas for the longest chain (**10NNpy**) the entropic contribution is approximately 50%. This trend clearly suggests that changes in entropy are responsible for the overall increase in $\Delta G^{\#}$, that is overrule the smaller contribution from the activation enthalpy. A possible reason for the increase in transition state order on increasing the aliphatic chain length, is the ability of the Pt(II) center to

dx.doi.org/10.1021/ic201151h |*Inorg. Chem.* 2011, 50, 8984–8996

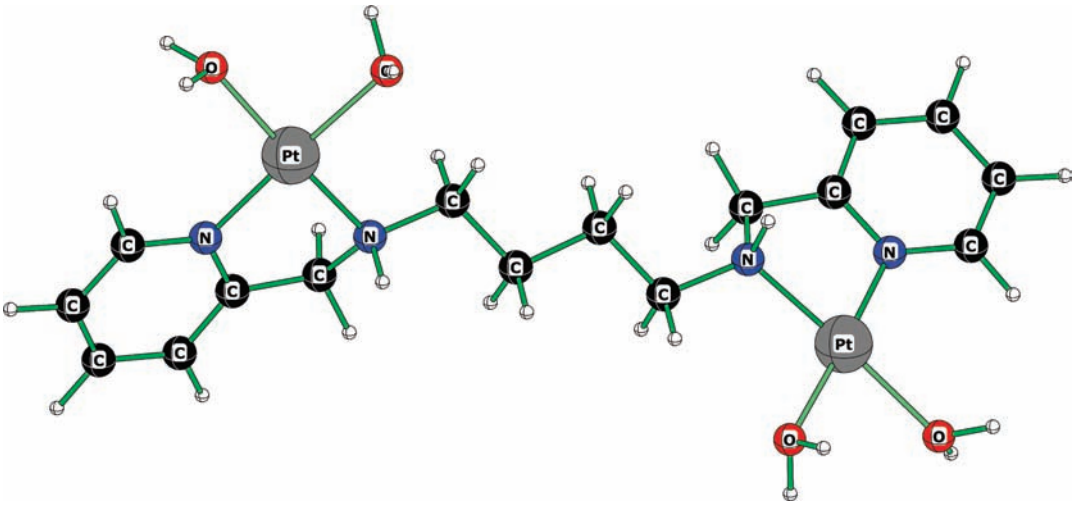

Figure 12. Calculated structure (C2) BP86/LCVP* of the **4NNpy** complex[51].

undergo a more effective reorganization when the second Pt(II) center is further away.

DFT Calculations. Table 3 summarizes the results of the quantum chemical calculations. The data show in general shorter Pt−N bonds than the Pt−O bonds. Furthermore, the Pt−N_{py} bond is shorter that the Pt−N_{amine} bond, which nicely supports our arguments in favor of a strong Pt−N_{py} bond resulting from the π−back bonding effect. The Pt−O bonds are very similar in both cases and show no clear preference for which coordinated water molecule is the more labile one. The calculated dihedral angels (N_{py}−Pt···Pt−N_{py}) indicate a twist in the ring arrangement. An analysis of the calculated Pt−Pt distances show that two additional CH_2 groups add 2.55 Å to the Pt−Pt distance, which is very similar to the results of Ertürk et al.[15] Figure 12 shows the **4NNpy** complex as an example for the calculated structures (also Figures S30−S32 of the Supporting Information).

CONCLUSIONS

In this study, a series of novel dinuclear Pt(II) complexes with bidentate nitrogen donor ligands and two vacant coordination sites were synthesized. Thereby, the effect of increasing the length of the aliphatic chain on the bridged complexes was studied. Determination of the pK_a values showed four acid dissociation steps. Because of the overall charge of 4+ on the complexes, the water ligands are more acidic compared to the mononuclear reference complex **monoNNpy**. Furthermore, a deprotonation pattern was established where the first and second steps occur trans to the pyridine unit. The difference between the pK_{a1} and pK_{a2} values, as well as between the pK_{a3} and pK_{a4} values, becomes smaller as the distance between the Pt(II) centers increases. This is assigned to an electrostatic interaction between the two Pt(II) centers, which becomes weaker on elongation of the chain. Kinetic measurements were performed with thiourea as a strong nucleophile. Because of the neutral character of the nucleophile, the overall charge does not change during the substitution reactions and two successive steps could be observed. It was found that the first reaction step, k_1, is independent of the chain length, because the driving force in this case is the strong π−acceptor ability of the pyridine ligand. In contrast, the second substitution step, k_2, depends on the chain length, because elongation of the chain leads to an electron donating effect, which results in a less electrophilic Pt(II) center that slows down the reaction. This study shows that it is necessary to balance the different donor abilities of the coordinated ligands to determine which effect predominates. We found that the π−acceptor pyridine overruled the σ−donor NHR_2 contribution and causedthe entering nucleophile to be stabilized in the position trans to the pyridine unit. The acceleration of the reactions by pressure and the significantly negative $\Delta V^{\#}$ values are typical for an associative substitution mechanism, which is also supported by the negative $\Delta S^{\#}$ values calculated from the temperature-dependent studies of the reaction.

In comparison to the dinuclear complexes prepared by Ertürk et al. (**(Ptpap)$_2$**, as seen in Figure 1), we note that the complexes synthesized in this study are significantly more stable because dechelation through displacement of the ring system by thiourea is indeed very slow and only starts after 24 h. The successive decomposition of the complexes was not investigated further. The fact that the prepared dinuclear systems show a high stability against nucleophilic attack by strong S-donor ligands is important, since sulfur-containing nucleophiles are overall present in cells and play an important role in biological reactions. On comparing the first substitution steps of **BBR3464** and **(Ptpap)$_2$** with this study, we found that with increasing number of π−acceptor ligands (zero, one and two), the rate constants k_1 increase in the order **BBR3464** (5.2 M^{-1} s^{-1})[20] < **NNpy** systems (52 M^{-1} s^{-1}) < **(Ptpap)$_2$** system (about 600 M^{-1} s^{-1})[16] using thiourea as a nucleophile. This can clearly be ascribed to the increase in the electrophilicity of the Pt(II) center on increasing the number of π−acceptor ligands. In such a way, the reactivity of the complex can be tuned in a systematic way, which could have an important effect on their antitumor efficiency because it is known that inside the cell many different nucleophiles can compete with the DNA (major target for the platinum drug) and furthermore intermediates with sulfur−donor nucleophiles such as methionine or glutathione can occur and are presumably responsible for several side effects.[52]

The above comparison is complicated by the fact that in some systems only one labile water ligand is coordinated to the metal center. However, nearly no related kinetic investigations of dinuclear complexes including two labile leaving groups were performed using common nucleophiles, for example chloride or

thiourea. Nevertheless, the (**2,2/c,c**) complex system of Farrell and his group[10] is very close to the dinuclear complexes used in this work. Indeed there are no kinetic data available for comparison, but Farrell et al. pointed out that during the reaction of 4 equivs of 5′-GMP (guanosine 5′-monophosphate), the final product had lost all four water ligands that were displaced by 5′-GMP nucleophiles.[10] This is comparable with the results found in this study, namely the complete displacement of water molecules by a nucleophile. Furthermore, the cytotoxicity of the complex system (**2,2/c,c**) was examined by Farrell et al. using murine L1210 leukemia cell lines.[11] As a result of these studies the bidentate complexes were found to be cytostatic active.[10,11] Finally, we conclude that bis(platinum) complexes with bidentate coordination spheres are promising compounds for antitumor active drugs.

■ ASSOCIATED CONTENT

Supporting Information. Mass spectra of the **10NNpy** complex; UV−vis spectra for the complexes **6NNpy**, **8NNpy**, **10NNpy** and **monoNNpy** in the pH range of 2−9 and plots of absorbance versus pH; different UV−vis specral changes, kinetic traces, concentration, temperature and pressure-dependent studies for all dinuclear complexes; calculated structures of the dinuclear complexes; table of a summary of the calculated pK_a values for the **4NNpy** complex; tables summarizing all values for k_{obs} determined for all reactions at different concentrations, temperatures, and pressures for all complexes. This material is available free of charge via the Internet at http://pubs.acs.org.

■ AUTHOR INFORMATION

Corresponding Author
*E-mail: vaneldik@chemie.uni-erlangen.de.

■ ACKNOWLEDGMENT

The authors gratefully acknowledge continued financial support from the Deutsche Forschungsgemeinschaft. The authors kindly thank Prof. Dr. Ivana Ivanović-Burmazović and Oliver Tröppner for their support with the mass spectrometric measurements.

■ REFERENCES

(1) Rosenberg, B.; VanCamp, L.; Trosko, J. E.; Mansour, V. H. *Nature* **1969**, *222*, 385–386.
(2) Lippert, B. *Cisplatin: Chemistry and Biochemistry of a Leading Anticancer Drug*; Wiley-VCH: Zürich, Switzerland, 1999.
(3) Wheate, N. J.; Walker, S.; Craig, G. E.; Oun, R. *Dalton Trans.* **2010**, *39*, 8113–8127.
(4) (a) Kelland, L. R. *Nat. Rev. Cancer* **2007**, *7*, 573–584. (b) Wong, E.; Giandomenico, C. M. *Chem. Rev.* **1999**, *99*, 2451–2466.
(5) (a) Eastman, A.; Schulte, N. *Biochemistry* **1988**, *27*, 4730–4734. (b) Fichtinger-Schepman, A. M. J.; van der Veer, J. L.; den Hartog, J. H. J.; Lohman, P. H. M.; Reedijk, J. *Biochemistry* **1985**, *24*, 707–713.
(6) (a) Jung, Y. W.; Lippard, S. J. *Chem. Rev.* **2007**, *107*, 1387–1407. (b) Ohndorf, U. M.; Rould, M. A.; He, Q.; Pabo, C. O.; Lippard, S. J. *Nature* **1999**, *399*, 708–712.
(7) Jakubec, M. A.; Galanski, M.; Keppler, B. K. *Rev. Physiol. Biochem. Pharmacol.* **2003**, *146*, 1–53.
(8) Farrell, N. *Comments Inorg. Chem.* **1995**, *16*, 373–389.
(9) Brabec, V.; Kasparkova, J.; Vrana, O; Novakova, O; Cox, J. W.; Qu, Y.; Farrell, N. *Biochemistry* **1999**, *38*, 6781–6790.
(10) Qu, Y; Farrell, N. *J. Am. Chem. Soc.* **1991**, *113*, 4851–4857.
(11) (a) Farrell, N; Qu, Y. *Inorg. Chem.* **1989**, *28*, 3416–3420. (b) Farrell, N.; de Almeida, S. G.; Skov, K. A. *J. Am. Chem. Soc.* **1988**, *110*, 5018–5019. (c) Farrell, N.; Qu, Y.; Hacker, M. P. *J. Med. Chem.* **1990**, *33*, 2179–2184. (d) Roberts, J. D.; Van Houten, B.; Qu, Y.; Farrell, N. P. *Nucleic Acids Res.* **1989**, *17*, 9719–9733. (e) Kraker, A.; Elliott, W.; Van Houten, B.; Farrell, N.; Hoeschele, J.; Roberts, J. *J. Inorg. Biochem.* **1989**, *36*, 160.
(12) Farrell, N.; Qu, Y.; Feng, L.; Van Houten, B. *Biochemistry* **1990**, *29*, 9522–9531.
(13) (a) Shah, N.; Dizon, D. S. *Future Oncology* **2009**, *5*, 33–42. (b) Hensing, T. A.; Hanna, N. H.; Gillenwater, H. H.; Gabriella Camboni, M.; Allievi, C.; Socinski, M. A. *Anticancer Drugs* **2006**, *17*, 697–704.
(14) (a) Cox, J. W.; Berners-Price, S. J.; Davies, M. S.; Qu, Y.; Farrell, N. *J. Am. Chem. Soc.* **2001**, *123*, 1316–1326. (b) Brabec, V.; Kasparova, J. *Drug Resist. Updates* **2005**, *8*, 131–146.
(15) Ertürk, H.; Hofmann, A.; Puchta, R.; van Eldik, R. *Dalton Trans.* **2007**, *22*, 2295–2301.
(16) Ertürk, H.; Maigut, J.; Puchta, R.; van Eldik, R. *Dalton Trans.* **2008**, *20*, 2759–2766.
(17) Bloemink, M. J.; Engelking, H.; Karentzopoulos, S.; Krebs, B.; Reedijk, J. *Inorg. Chem.* **1996**, *35*, 619–627.
(18) Grehl, M.; Krebs, B. *Inorg. Chem.* **1994**, *33*, 3877–3885.
(19) (a) Cleare, M. J.; Hoeschele, J. D. *Platinum Met. Rev.* **1973**, *17*, 3–7. (b) Cleare, M. J.; Hoeschele, J. D. *Platinum Met. Rev.* **1973**, *2*, 187–210.
(20) Summa, N.; Maigut, J.; Puchta, R.; van Eldik, R. *Inorg. Chem.* **2007**, *46*, 2094–2104.
(21) Hureau, C.; Blondin, G.; Charlot, M.-F.; Philouze, C.; Nierlich, M.; Cesario, M.; Anxolabehere-Mallart, E. *Inorg. Chem.* **2005**, *44*, 3669–3683.
(22) Hofmann, A.; van Eldik, R. *Dalton Trans.* **2003**, *15*, 2979–2985.
(23) van Eldik, R.; Gaede, W.; Wieland, S.; Kraft, J.; Spitzer, M.; Palmer, D. A. *Rev. Sci. Instrum.* **1993**, *64*, 1355–1357.
(24) (a) Becke, A. D. *J. Chem. Phys.* **1993**, *98*, 5648–5652. (b) Lee, C.; Yang, W.; Parr, R. G. *Phys. Rev. B: Condens. Matter* **1988**, *37*, 785–789. (c) Stephens, P. J.; Devlin, F. J.; Chabalowski, C. F.; Frisch, M. J. *J. Phys. Chem.* **1994**, *98*, 11623–11627.
(25) (a) Dunning, T. H.; Hay, P. J. *Modern Theoretical Chemistry*; Vol. 3, pp 1−28, Plenum, New York; 1976. (b) Hay, P. J.; Wadt, W. R. *J. Chem. Phys.* **1985**, *82*, 270–283. (c) Wadt, W. R.; Hay, P. J. *J. Chem. Phys.* **1985**, *82*, 284–298. (d) Hay, P. J.; Wadt, W. R. *J. Chem. Phys.* **1985**, *82*, 299–310.
(26) Gilson, R .; Durrant, M. C. *Dalton Trans.* **2009**, *46*, 10223–10230.
(27) (a) Miertus, S.; Scrocco, E.; Tomasi, J. *Chem. Phys.* **1981**, *55*, 117–129. (b) Miertus, S.; Tomasi, J. *Chem. Phys.* **1982**, *65*, 239–245. (c) Cossi, M.; Barone, V.; Cammi, R.; Tomasi, J. *Chem. Phys. Lett.* **1996**, *255*, 327–335. (d) Cancès, M. T.; Mennucci, B.; Tomasi, J. *J. Chem. Phys.* **1997**, *107*, 3032–3041. (e) Barone, V.; Cossi, M.; Tomasi, J. *J. Chem. Phys.* **1997**, *107*, 3210–3221. (f) Cossi, M.; Barone, V.; Mennucci, B.; Tomasi, J. *Chem. Phys. Lett.* **1998**, *286*, 253–260. (g) Barone, V.; Cossi, M.; Tomasi, J. *J. Comput. Chem.* **1998**, *19*, 404–417. (h) Barone, V.; Cossi, M. *J. Phys. Chem. A* **1998**, *102*, 1995–2001. (i) Mennucci, B.; Tomasi, J. *J. Chem. Phys.* **1997**, *106*, 5151–5158. (j) Mennucci, B.; Cancès, E.; Tomasi, J. *J. Phys. Chem. B* **1997**, *101*, 10506–10517. (k) Tomasi, J.; Mennucci, B.; Cancès, E. *J. Mol. Struct. (Theochem)* **1999**, *464*, 211–226. (l) Cammi, R.; Mennucci, B.; Tomasi, J. *J. Phys. Chem. A* **1999**, *103*, 9100–9108. (m) Cossi, M.; Barone, V.; Robb, M. A. *J. Chem. Phys.* **1999**, *111*, 5295–5302. (n) Cammi, R.; Mennucci, B.; Tomasi, J. *J. Phys. Chem. A* **2000**, *104*, 5631–5637. (o) Cossi, M.; Barone, V. *J. Chem. Phys.* **2000**, *112*, 2427–2435. (p) Cossi, M.; Barone, V. *J. Chem. Phys.* **2001**, *115*, 4708–4717. (q) Cossi, M.; Rega, N.; Scalmani, G.; Barone, V. *J. Chem. Phys.* **2001**, *114*, 5691–5701. (r) Cossi, M.; Scalmani, G.; Rega, N.; Barone, V. *J. Chem. Phys.* **2002**, *117*, 43–54.
(28) (a) Slater, J. C. *Quantum Theory of Molecules and Solids, Vol. 4: The Self-Consistent Field for Molecules and Solids*; McGraw-Hill, New York, 1974. (b) Perdew, J. P.; Zunger, A. *Phys. Rev. B: Condens. Matter* **1981**, *23*, 5048–5079. (c) Perdew, J. P. *J. Phys. Rev. B: Condens. Matter* **1986**, *33*, 8822–8824.

(29) (a) Ditchfield, R.; Hehre, W. J.; Pople, J. A. *J. Chem. Phys.* **1971**, *54*, 724–728. (b) Hehre, W. J.; Ditchfield, R.; Pople, J. A. *J. Chem. Phys.* **1972**, *56*, 2257–2261. (c) Hehre, W. J.; Pople, J. A. *J. Chem. Phys.* **1972**, *56*, 4233–4234. (d) Hariharan, P. C.; Pople, J. A. *Theor. Chim. Acta* **1973**, *28*, 213–222. (e) Binkley, J. S.; Pople, J. A. *J. Chem. Phys.* **1977**, *66*, 879–880. (f) Francl, M. M.; Pietro, W. J.; Hehre, W. J.; Binkley, J. S.; Gordon, M. S.; DeFrees, D. J.; Pople, J. A. *J. Chem. Phys.* **1982**, *77*, 3654–3665.

(30) (a) Dunlap, B. I. *J. Chem. Phys.* **1983**, *78*, 3140–3142. (b) Dunlap, B. I. *J. Mol. Struct. (Theochem)* **2000**, *529*, 37–40.

(31) Frisch, M. J.; Trucks, G. W.; Schlegel, H. B.; Scuseria, G. E.; Robb, M. A.; Cheeseman, J. R.; Montgomery Jr., J. A.; Vreven, T.; Kudin, K. N.; Burant, J. C.; Millam, J. M.; Iyengar, S. S.; Tomasi, J.; Barone, V.; Mennucci, B.; Cossi, M.; Scalmani, G.; Rega, N.; Petersson, G. A.; Nakatsuji, H.; Hada, M.; Ehara, M.; Toyota, K.; Fukuda, R.; Hasegawa, J.; Ishida, M.; Nakajima, T.; Honda, J.; Kitao, O.; Nakai, H.; Klene, M.; Li, X.; Knox, J. E.; Hratchian, H. P.; Cross, J. B.; Bakken, V.; Adamo, C.; Jaramillo, J.; Gomperts, R.; Stratmann, E.; Yazyev, O.; Austin, A. J.; Cammi, R.; Pomelli, C.; Ochterski, J. W.; Ayala, P. Y.; Morokuma, K.; Voth, G. A.; Salvador, P.; Dannenberg, J. J.; Zakrzewski, V. G.; Dapprich, S.; Daniels, A. D.; Strain, M. C.; Farkas, O.; Malick, D. K.; Rabuck, A. D.; Raghavachari, K.; Foresman, J. B.; Ortiz, J. V.; Cui, Q.; Baboul, A., G.; Clifford, S.; Cioslowski, J.; Stefanov, B. B.; Liu, G.; Liashenko, A.; Piskorz, P.; Komaromi, I.; Martin, R. L.; Fox, D. J.; Keith, T.; Al-Laham, M. A.; Peng, C. Y.; Nanayakkara, A.; Challacombe, M.; Gill, P. M. W.; Johnson, B.; Chen, W.; Wong, M. W.; Gonzalez, C.; Pople, J. A. *Gaussian 03, Rev. B.03*; Gaussian Inc., Wallingford, CT, 2004.

(32) Coley, R. F.; Martin, D. S. *Inorg. Chim. Acta* **1973**, *7*, 573–577.

(33) Berners-Price, S. J.; Frenkiel, T. A.; Frey, U.; Ranford, J. D.; Sadler, P. J. *J. Chem. Soc., Chem. Commun.* **1992**, *10*, 789–791.

(34) Barton, S. J.; Barnham, K. J.; Habtemariam, A.; Sue, R. E.; Sadler, R. J. *Inorg. Chim. Acta* **1998**, *273*, 8–13.

(35) Hofmann, A.; Jaganyi, D.; Munro, O. Q.; Liehr, G.; van Eldik, R. *Inorg. Chem.* **2003**, *42*, 1688–1700.

(36) Summa, N.; Schiessl, W.; Puchta, R.; van Eikema Hommes, N.; van Eldik, R. *Inorg. Chem.* **2006**, *45*, 2948–2959.

(37) Hofmann, A.; van Eldik, R. *Dalton Trans.* **2003**, *15*, 2979–2985.

(38) Davies, M. S.; Cox, J. W.; Berners-Price, S. J.; Barklage, W.; Qu, Y; Farrell, N. *Inorg. Chem.* **2009**, *39*, 1710–1715.

(39) (a) Lee, K. W.; Martin, D. S. *Inorg. Chim. Acta* **1976**, *17*, 105–110. (b) Lim, M. C.; Martin, R. B. *J. Inorg. Nucl. Chem.* **1976**, *38*, 1911–1914. (c) Faggiani, R.; Lippert, B.; Lock, C. J. L.; Rosenberg, B. *J. Am. Chem. Soc.* **1977**, *99*, 777–781.

(40) Reedijk, J. *Eur. J. Inorg. Chem.* **2009**, *10*, 1303–1312.

(41) Fallis, S.; Anderson, G. K.; Rath, N. P. *Organometallics* **1991**, *10*, 3180–3184.

(42) Mahal, G.; van Eldik, R. *Inorg. Chem.* **1985**, *24*, 4165–4170.

(43) Mahal, G.; van Eldik, R. *Inorg. Chem.* **1987**, *127*, 203–208.

(44) Tobe, M. L.; Burgess, J. *Inorganic Reaction Mechanism*; Adison Wesley Longman Limited; 1999, Chapter 3, 46−127.

(45) Stochel, G.; van Eldik, R. *Coord. Chem. Rev.* **1999**, *187*, 329–374.

(46) Helm, L.; Elding, L. I.; Merbach, A. E. *Helv. Chim. Acta* **1984**, *67*, 1453–1460.

(47) Helm, L.; Elding, L. I.; Merbach, A. E. *Helv. Chim. Acta* **1985**, *24*, 1719–1721.

(48) Wendt, O. F.; Elding, L. I. *J. Chem. Soc., Dalton Trans.* **1997**, *24*, 4725–4731.

(49) Wendt, O. F.; Elding, L. I. *Inorg. Chem.* **1997**, *36*, 6028–6032.

(50) Otto, S.; Elding, L. I. *J. Chem. Soc., Dalton Trans.* **2002**, 2354–2360.

(51) The performance of this computational level is well documented; see, e.g.: (a) Müller, R.; Hübner, E.; Burzlaff, N. *Eur. J. Inorg. Chem.* **2004**, *10*, 2151–2159. (b) Peters, L.; Hübner, E.; Burzlaff, N. *J. Organomet. Chem.* **2005**, *690*, 2009–2016. (c) Scheurer, A.; Puchta, R.; Hampel, F. *J. Coord. Chem.* **2010**, *63*, 2868–2878. (d) Ertürk, H.; Puchta, R.; van Eldik, R. *Eur. J. Inorg. Chem.* **2009**, *10*, 1331–1338.

(52) Reedijk, J. *Chem. Rev.* **1999**, *99*, 2499–2510.